Chinese Journal of Natural Medicines

Luteolin ameliorates ulcerative colitis in mice *via* reducing the depletion of NCR$^+$ILC3 through Notch signaling pathway

Xueqian XIE, Pengcheng LI, Meng ZHAO, Bo XU, Guixing ZHANG, Qing WANG, Chen NI, Xia LUO, Lian ZHOU

Citation: Xueqian XIE, Pengcheng LI, Meng ZHAO, Bo XU, Guixing ZHANG, Qing WANG, Chen NI, Xia LUO, Lian ZHOU, Luteolin ameliorates ulcerative colitis in mice *via* reducing the depletion of NCR$^+$ILC3 through Notch signaling pathway, Chinese Journal of Natural Medicines, 2024, 22(11), 1−13. doi: 10.1016/S1875−5364(24)60568−6.

View online: https://doi.org/10.1016/S1875−5364(24)60568−6

Available online at www.sciencedirect.com
ScienceDirect
Chinese Journal of Natural Medicines 2024, **22**(11): 991-1002
doi: 10.1016/S1875-5364(24)60568-6
Chinese Journal of Natural Medicines

•Original article•

Luteolin ameliorates ulcerative colitis in mice *via* reducing the depletion of NCR$^+$ILC3 through Notch signaling pathway

XIE Xueqian[1], LI Pengcheng[1], ZHAO Meng[1], XU Bo[1], ZHANG Guixing[2], WANG Qing[1], NI Chen[1], LUO Xia[1*], ZHOU Lian[1*]

[1] *School of Pharmaceutical Sciences, Guangzhou University of Chinese Medicine, Guangzhou 510000, China;*
[2] *Shenzhen Bao'an Traditional Chinese Medicine Hospital, Guangzhou University of Chinese Medicine, Shenzhen 518000, China*

Available online 20 Nov., 2024

[ABSTRACT] The disorder of group 3 innate lymphoid cells (ILC3) subgroup, such as the predominance of NCR$^-$ILC3 but the depletion of NCR$^+$ILC3, is unfavorable to damaged intestinal barrier repair, which leads to the prolongations and obstinacy of ulcerative colitis (UC). Our previous studies had shown that luteolin promoted NCR$^-$ILC3 differentitating into NCR$^+$ILC3 to improving the depletion of NCR$^+$ILC3 in UC mice, while the mechanism is unclear. This article aimed to explore the underlying mechanism of luteolin enhancing the proportion NCR$^+$ILC3. UC mice model was established with 2% DSS and Notch signaling was blocked, then luteolin was used to intervene. The results showed that the effect of luteolin on ameliorating disease symptoms in UC mice, including inhibiting the weight loss, reducing the pathological damage of colon mucosa, *etc.*, was diminished with blocking Notch signaling pathway. In addition, luteolin increased the proportion of NCR$^+$ILC3, NCR$^+$MNK3 and IL-22$^+$ILC3, decreased intestinal permeability, promoted mucin secretion, and promoted ZO-1 and Occludin expression, the above effect of luteolin was neutralized by Notch inhibitor LY-411575. Luteolin activated the abnormally blocked Notch signaling pathway in UC mice. And molecular docking predicted the affinity of luteolin for RBPJ to be −7.5 kcal·mol^{-1} in mouse, respectively; the affinity of luteolin for Notch1 and RBPJ was respectively scored to be −6.4 kcal·mol^{-1} and −7.7 kcal·mol^{-1} homo sapiens. These results proved that luteolin is positive for enhancing the proportion of NCR$^+$ILC3 *via* Notch signaling, and it provides a basis for targeting NCR$^+$ILC3 for restoring intestinal barrier function to alleviating ulcerative colitis.

[KEY WORDS] Luteolin; Ulcerative colitis; Group 3 innate lymphoid cells; Notch1; RBPJ
[CLC Number] R965 **[Document code]** A **[Article ID]** 2095-6975(2024)11-0991-12

Introduction

Ulcerative colitis (UC) is a multifactorial refractory autoimmune disease characterized by mucosal inflammation that begins in the rectum and continues to extend to the proximal colon [1]. The therapeutic strategy of UC mainly focuses on inhibiting the inflammation of the damaged mucosal [2]. But, this treatment principle fails to solve the tough problem of colitis symptom persistence. Recently, studies have proposed that restoring the integrity of intestinal mucosal epithelium could solve this problem in UC [3].

The intestinal mucosal barrier is the first defense line of the intestine. Physiologically, a fully functional intestinal mucosal barrier blocks the toxins, bacteria and viruses away to avoiding the overactivation of the immune system [4]. Mucosal barrier destruction is the basic pathological feature of UC, intestinal mucosal permeability increases and intestinal antigen activates intestinal-mucosal immune cells [5]. Furthermore, this abnormal immune system breaks intestinal immune tolerance, even causes symbiotic microbial disorders, which will eventually incur intestinal epithelial damage, or make the damaged mucosa unfavorable to repair, resulting in repeated attacks of UC [6].

Interleukin-22 (IL-22) is currently recognized as an important regulator of intraepithelial environmental homeostasis [7-8]. IL-22 is mainly derived from group 3 innate lymphoid cells (ILC3) [9]. According to the expression of chemokine (C-C motif) receptor 6 (CCR6), ILC3 can be divided into two subtypes: CCR6$^-$ILC3 and CCR6$^+$ILC3. CCR6$^-$ILC3

[Received on] 23-Feb.-2024
[Research funding] This work was supported by the National Natural Science Foundation of China (No. 82074092), the Natural Science Foundation of Guangdong Province (No. 2021A1515012219) and Guangzhou University of Chinese Medicine "Double First-Class" and High-level University Discipline Collaborative Innovation Team Project (No. 2021xk81).
[*Corresponding author] E-mails: luoxia@gzucm.edu.cn (LUO Xia); zl@gzucm.edu.cn (ZHOU Lian)
These authors have no conflict of interest to declare.

was further including two subtypes according to natural cytotoxicity receptor (NCR): $NCR^{-}CCR6^{-}ILC3$ and $NCR^{+}CCR6^{-}ILC3$. The former can secrete a large amount of Interleukin-17a (IL-17a), while the latter mainly secretes IL-22. $NCR^{+}ILC3$ is closely related to mucosal repair [10], which is differentiated from $NCR^{-}ILC3$ *via* Notch signal pathway [11].

In UC mice and UC patients, the $NCR^{+}ILC3$ population decreased [12-13]. The imbalance of ILC3 subsets resulted in a tilt in their effector cytokine levels and a decrease in IL-22 levels. Since ILC3-derived IL-22 is closely crucial to the promotion of intestinal mucosal repair, for the most part, $NCR^{+}ILC3$ determines the level of IL-22 in the intestinal lamina propria, the maintenance of intestinal $NCR^{+}ILC3$ homeostatic is beneficial to the repair of damaged mucosal.

Luteolin (3,4,5,7-tetrahydroxy flavone) exists in Dahuang Mudan Decoction [14] and has a variety of pharmacological effects, such as anti-inflammatory, anti-allergic, antitumor, antiviral, immune regulation and so on. In our previous study, we determined that Dahuang Mudan Decoction and luteolin showed respectable therapeutic effect in UC mice [15]. It was also found that luteolin promoted the differentiation of $NCR^{-}ILC3$ to $NCR^{+}ILC3$ in UC mice, thereby maintaining the proportion of $NCR^{+}ILC3$ and promoting the repair of damaged intestinal mucosa in UC mice. Moreover, the results of *in vitro* experiments showed that luteolin enhanced the proportion of $NCR^{+}MNK3$ *via* Notch signaling [16]. However, whether the mechanism by which luteolin enhancing the proportion of $NCR^{+}ILC3$ *in vivo* depends on Notch signaling and the role of Notch signaling pathway in UC remains unclear. Therefore, in this article, we focus on exploring the mechanism of luteolin effecting on $NCR^{+}ILC3$ *in vivo*.

Materials and Methods

Drugs and reagents

Dextranan sulfate (DSS) was purchased from MP Biomedicals (CA, USA), dissolved in sterile water to obtain 2% Dss solution; Luteolin (≥ 98% purity) was purchased from Yuanye Biological Technology Co., Ltd. (Shanghai, China), dispersed in 0.5% sodium carboxymethylcellulose (CMC-Na) to obtain 0.5 $mg \cdot mL^{-1}$ luteolin solution; CMC-Na was was purchased from Solarbio (Beijing, China, dissolved in hot water); Hes1 (D6P2U) Rabbit mAb was purchased from CST (1 : 1000, Boston, MA, USA); Anti-Notch1 antibody, Anti-ZO-1 antibody and Anti-Occludin antibody was purchased from abcam (1 : 1000, Cambridge, UK); c-Myc was obtained from AbMART (1 : 2000, Shanghai China); Goat Anti-Mouse IgG H&L (HRP) and Goat Anti-Rabbit IgG H&L (HRP) were purchased from Bei jing Bioss Biotechnology Co., Ltd. (1 : 3000, Beijing, China); APC anti-mouse NCR, APC anti-mouse IL-17A Antibody, and PE anti-mouse IL-22 Antibody and Alexa Fluor 700 anti-mouse CD45 were purchased from BioLegend (Calif., USA), all above antibodies were diluted according to the recommended concentration in the instructions; Alcian Blue & Nuclear Fast Red Staining Kit (pH2.5) was obtained from Beyotime Biotechnology Co., Ltd. (Shanghai, China); Fluorescein TSA Fluorescence System Kit and Cy3 TSA Fluorescence System Kit were purchased from APExBIO Technology (HOU, USA); LY-411575 was obtained from MCE(New Jersey, USA) [17]; Mouse IL-22, IL-17A, LPS enzyme-linked immunosorbent assay (ELISA) kits were obtained from Jiangsu Enzyme Industry Co., Ltd. (Jiangsu, China).

Animal treatment

70 C57BL/6J mice (specific pathogen-free, male, 6−8 week of age, weight 20−22 g) were purchased from Guangdong Zhiyuan Biomedical Technology Co., Ltd. (Guangzhou, China). The mice were housed under specific pathogen-free conditions, at 40%−80% humidity, a temperature of 24 ± 1 °C, and a 12h light/dark cycle. All animal experimental procedures were approved by the Laboratory Animal Welfare and Ethics Committee, School of Pharmaceutical Sciences, Guangzhou University of Chinese Medicine. (No. ZYD-2022-061).

After the end of adaptive feeding, the mice were randomly divided into 5 groups: control group, model group, luteolin group (10 $mg \cdot kg^{-1}$), Notch inhibitor (LY-411575) group (LY group, 2 $mg \cdot kg^{-1}$ [18]) and LY-411575 (2 $mg \cdot kg^{-1}$) + luteolin group (10 $mg \cdot kg^{-1}$). The control group was given distilled water, and the other groups were treated with DSS to drink freely for 5 days, and then replaced with distilled water for 4 days, a total of four rounds to induce the UC model. In the inhibitor group, Notch inhibitor (LY-411575) was intraperitoneally injected at the first day of model, and the other groups were also intraperitoneally injected with solvent. After the first round of model, the normal group, the inhibitor group and the model group were intragastric with 0.5% CMC-Na every day, the luteolin group and the inhibitor + luteolin group were oral medication with luteolin every day for a total of 31 days. The mice were sacrificed on day 37, there were 12−14 mice survival each group, 6 mice were randomly selected for Flow cytometry analysis, the remaining mice were used for Western blot, Immunofluorescence, Small animal imaging and so on. (see Fig. 1 for specific methods).

Disease activity index (DAI)

The weight of the mice was weighed and recorded every day. Mice faeces were collected at least twice in one modeling cycle, and the characteristics of feces were recorded. Occult blood levels in mice feces were evaluated using occult blood kits. Combined with body weight, fecal traits and fecal occult blood condition, DAI score was performed [14].

Colon length, thymus index and spleen index

On the 37th day of the experiment, the mice were anesthetized with carbon dioxide (CO_2) for orbital blood extraction and then sacrificed. The natural extension length of the colons was measured and photographed. Spleen and thymus of mice were weighed and recorded, and spleen index and thymus index were calculated [14].

Hematoxylin and eosin (H&E) kits

The mucosal inflammation in UC begins in the rectum

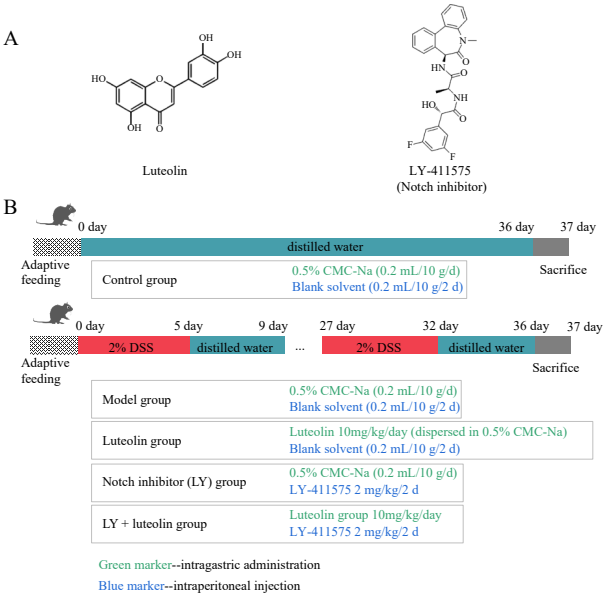

Fig. 1 Establishment of ulcerative colitis mouse model. A, Chemical Structures of Luteolin and LY-411575 B, Administration schedule.

and continues to extend to the colon, In order to exclude the effect of different positions of the colon on the experimental results, consistently, the colon segment 2 cm from the mouse anus (about 1.5 cm) was cut out and soaked in 4% paraformaldehyde for later use. After dehydration, embedding, and finally we used paraffin slicer to slice the tissue into 4 μm sections. Hematoxylin and eosin (H&E) kits were used to stain Sections, the cytoplasm is stained light red and the nucleus appears blue. And the microscopic vision of colon were observed with a microscope (Olympus, Japan) at 200 × &630 × magnification.

Peripheral blood analysis of mice

20 μL of mouse peripheral blood was taken and mixed in an anticoagulant tube containing 0.1% heparin sodium solution to ensure that there were no clumps, and then Veterinary blood cell analyzer (Mindray Biomedical Electronics Co., Ltd., Shenzhen BC-2800Vet) was used to detect the level of white blood cells (WBC) and red blood cells (RBC), the proportion of monocytes (Mon%), granulocyte (Gran%), lymphocytes (Lymph%), and hemoglobin (HGB) content in peripheral blood of mice.

Small animal imaging

On the 35th day of modeling, two mice were randomly selected from each group. After fasting for 12 h. The FITC-Dextran powder was prepared into a FITC-Dextran solution with a concentration of 2.5 mg·mL^{-1} using sterile water. The mice were intragastric administrated at 0.2 mL/10g (50 mg·kg^{-1}). Four hours later, the distribution of FITC-Dextran in the intestines of the mice was observed with small animal imaging system (NIGHT OWL LB 983, Germany).

Alcian blue & nuclear fast red staining

Alcian blue & nuclear fast red staining kit (Beyotime) was used to detected the mucin in colon according to the instructions.

Immunofluorescence

Using the TSA Fluorescence System Kit (ApexBio), the tight junction protein was examined and visualized by using immunofluorescence microscopy. Basically, the colon tissue was stained with rabbit anti-Occludin mAb (1 : 200 dilution, abcam), rabbit anti-ZO-1 mAb (1 : 200 dilution, abcam), rabbit anti-Hes1 antibody (CST, 1 : 200 dilution), rabbit anti-Notch1 antibody (abcam, 1 : 100 dilution), and goat anti-rabbit-HRP (Bioss,1 : 200) were used as secondary antibody. TSA amplification was then performed with FITC/cy3 tyramide and cell nucleus (DNA) was marked with DAPI (Solarbio), finally fluorescence microscopy was used to observe the fluorescence distribution of proteins in colon.

Western blot

Nuclear and Cytoplasmic Protein Extraction Kit (Beyotime, China) was used for obtaining colon tissues protein, and then electrophoresis to separating the proteins in 10% or 12% SDS-PAGE (load is 40 μg protein) and transferred onto PVDF membranes (0.45 μm). Membranes were treated with 5% skim milk and incubated with the primary antibody (ZO-1, Occludin, Notch1, Hes1, c-Myc, and β-actin) at 4 °C for 12 h. Membranes were washed with TBS and incubated with an HRP conjugated secondary antibody for 1 h at room temperature. Proteins were visualized using ECL substrate and determined using ImageJ software.

Flow cytometry

The method of obtaining single-cell suspension is referred to the literature [14]. Cells were divided equally into two. Cells were incubated with Surface labeled antibody for 30 minutes at room temperature in the dark. After that, cells were dealed with FIX&PERM Cell Immobilization/Permeation Kit (Thermo Scientific) for 40 minutes, which conduced to antibodies permeate into the intracellular while ensuring none impact on morphological scattering properties of cells. Then, the cells were stained with intracellular labeled antibody. The first flow cytometry staining strategy: Lineage$^-$CD45$^+$RORgammat$^+$NCR$^+$; The second flow cytometry staining strategy: Lineage$^-$CD45$^+$RORgammat$^+$IL-17a$^+$/IL-22$^+$. Finally, BD LSR Fortessa was used to examine.

Cell experiment

We used the MNK3 cell line, which expresses ILC3-associated signaling transcription factors, cytokines, adhesion molecules, and chemokine receptors, and is considered to be an in vitro study system for ILC3.

MNK3 cells were obtained from Bluefbio Biology Technology Development Co., Ltd. (Shanghai, China). DMEM medium containing 10% fetal bovine serum and 1% penicillin/streptomycin was incubated in 5% CO_2 at 37 °C.

MNK3 cells were divided into four groups: Control group, inhibitor group (2 μmol·L^{-1} [19]), luteolin group (LY, 3.125 μmol·L^{-1}), and inhibitor + luteolin group. All drugs were incubated with MNK3 cells for 24 h.

Protein–ligand docking and interaction profiling

From the PubChem database (https://pubchem.ncbi.

nlm.nih.gov/) to determine the composition of the active compounds in name, molecular weight, download the 3D structures for mouse musculus RBPJ [PDB ID: 3IAG [20]], homo sapiens RBPJ [PDB ID: 6WQU [21]] and homo sapiens Notch1 [PDB ID: 4CUD [22-23]] from the RCSB PDB database (http://www.rcsb.org/). Then, AutoDock software was used to prepare ligands and proteins required for molecular docking. For the target protein, its crystal structure removed water molecules, hydrogenated, modified amino acids, optimized energy and adjusted force field parameters, and then, the low energy conformation satisfying the ligand structure is obtained.

Statistical analysis

Statistical analysis of data was carried out by GraphPad Prism software v8.3.0 software. The homogeneity test of variance was carried out for those conforming to normal distribution, multiple groups of data meeting the homogeneity of variance were tested by the analytical Dunnett method in one-way variance, while those not meeting the homogeneity of variance were tested by Dunnett's T3. The non-parametric Kruskal-Wallis test is used to compare the data of multiple independent samples that do not conform to the normal distribution and the homogeneity of variance. $P < 0.05$ was considered statistically significant.

Results

Non-redundant role of Notch signaling pathway in luteolin treated UC mice

Effectiveness is the basis for the mechanism of action. We first investigated the role of Notch signaling pathway in the treatment of UC mice with luteolin. Blocking Notch pathway did not worsen the weight loss and DAI score increase in UC mice, but impaired the effects of luteolin (Figs. 2A and 2B). The results of colon length and spleen index showed that blocking Notch pathway had no effect on colon length shortening and spleen enlargement in UC mice, but aggravated thymus atrophy. The effects of luteolin on restoring colon length and alleviating spleen enlargement and thymus atrophy in UC mice were weakened (Figs. 2C−2E). In addition, the colon glandular arrangement of UC mice was disordered or even disappeared, with a large number of inflammatory cell infiltrates. After treatment with luteolin, the inflammatory infiltration was reduced, and the glands partially recovered, while blocking Notch signaling pathway did not aggravate the above situation, but the effect of luteolin was neutralized. These results suggest that Notch signaling plays an indispensable role in the effect of luteolin on the improvement of UC mice related disease symptoms.

Analysis of peripheral blood cells in UC mice and intervention of luteolin

Peripheral blood of mice was detected by veterinary blood cell analyzer. The results showed that the number of white blood cells (WBC), the proportion of monocytes (Mon%) and granulocyte (Gran%) in the peripheral blood of UC mice increased significantly, while the proportion of lymphocytes (Lymph%), the number of red blood cells (RBC) and the content of hemoglobin (HGB) decreased significantly. After luteolin treatment, the number of WBC, Mon% and Gran% in the peripheral blood of UC mice could be reduced, and Lymph%, RBC and HGB is increased (Fig. 3). However, after Notch signaling pathway was blocked, there was no significant effect on Mon%, Gran%, Lymph%, WBC number, RBC number and HGB content in UC mice (Fig. 3A), but the above effect of luteolin was reversed. These results suggest that luteolin improves the level of peripheral inflammation and anemia in UC mice depending on Notch signaling pathway.

Blocking the Notch signaling pathway prevents luteolin from repairing damaged intestinal barrier

The barrier destruction caused by mucosal ulcer is the basic pathological change of UC. So, we next investigated the effect of Notch pathway and luteolin on damaged intestinal mucosa in UC mice. Results of small animal imaging showed that FITC-dextran fluorescence intensity of UC mice and Notch inhibitor-treated UC mice increased at the colon, indicating increased colon permeability, besides, the content of LPS in UC mice was increased, which indicated that the intestinal barrier was impaired and colon permeability increased, and luteolin reduced colon permeability of UC mice (Figs. 4A−4B). The results of Alcian blue staining showed that luteolin increased the mucin content (the area of blue region) in the colon of UC mice (Fig. 4C); HE staining results also showed that luteolin enhanced the number of goblet cells in UC mice (Fig. 2G). Multiple immunofluorescence and WB results showed that the expression of tight junction proteins ZO-1 and Occludin in colon of UC mice and UC mice treated with Notch inhibitor decreased, while the expression of ZO-1 and Occludin in UC mice treated with luteolin increased (Figs. 4D−4I). After blocking Notch signaling in UC mice, the favour of luteolin on intestinal barrier function was greatly neutralized.

luteolin restored NCR^+ILC3 proportion in UC mice via Notch signaling

It had been confirmed that luteolin was favourable for intestinal barrier function in UC mice, and then we researched into its mechanism. IL-22 is currently recognized as an important regulatory factor that promote the repair of the impaired intestinal barrier, and IL-22 in the intestine is mainly derived from ILC3, especially the NCR^+ILC3, which is a powerful source of IL-22. Multiple immunofluorescence was used to identify $ROR\gamma t^+NCR^+$cells in the colon (Supplementary Fig.1). Results showed that the proportion of ILC3 had no significant difference, but the proportion of NCR^+ILC3 and $IL\text{-}22^+$ILC3 in UC mice decreased significantly, which increased significantly after luteolin treatment, while these effects of luteolin were weakened after Notch inhibitor treatment (Figs. 5A−5F). These results suggest that the maintenance of NCR^+ILC3 and $IL\text{-}22^+$ILC3 by luteolin is dependent on Notch signaling pathway. It is worth noting that the pro-

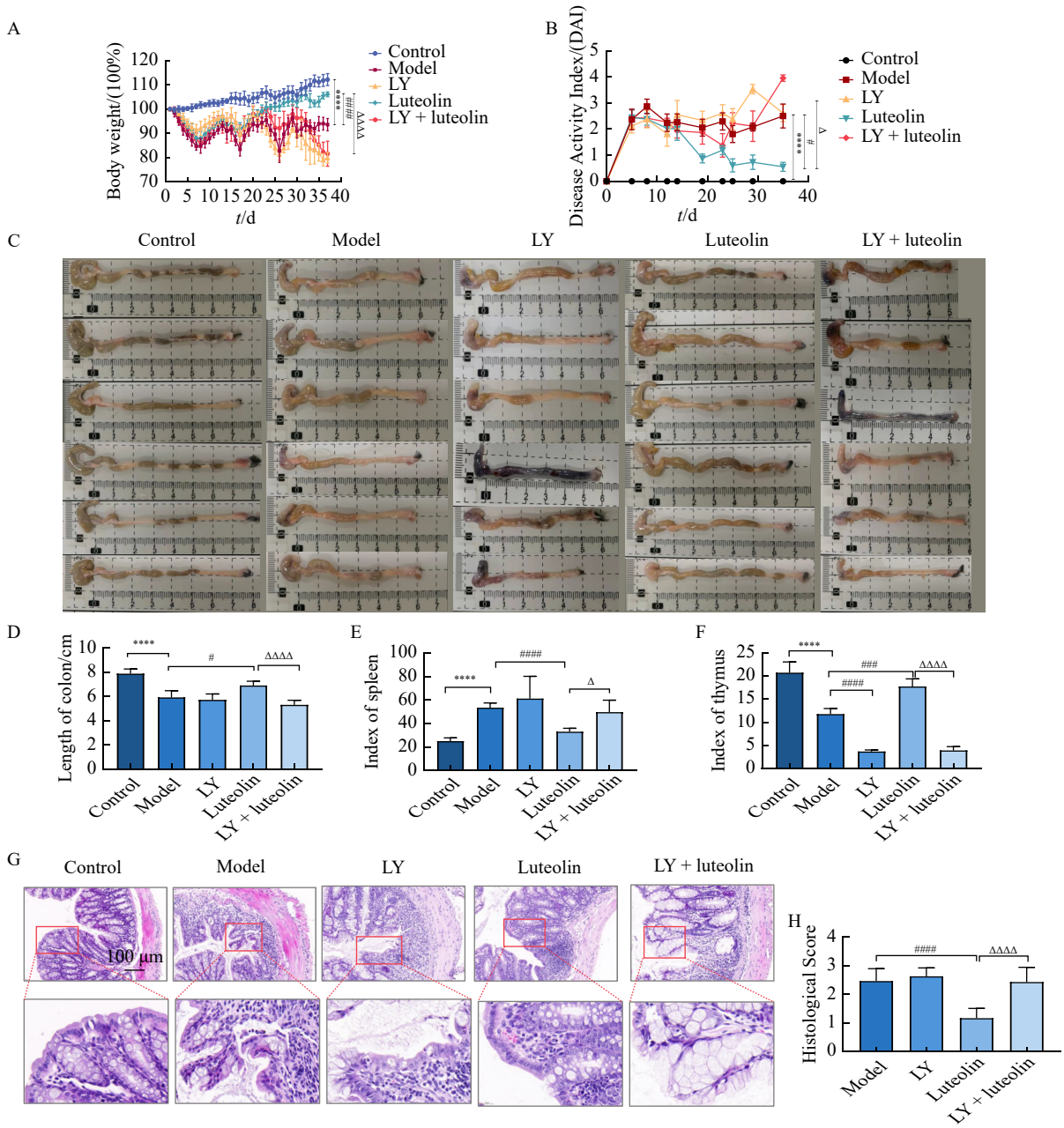

Fig. 2 Non-redundant role of Notch signaling pathway in luteolin treated UC mice. A, body weight ($n \geq 10$); B, DAI score ($n \geq 10$); C&D, Colon length ($n = 6$); E, Spleen index ($n = 6$); F, Thymus index ($n = 6$); G, H&E staining of colon tissue (200 ×&630 × magnification, $n = 6$); H, Histological score ($n = 6$). LY, Notch inhibitor, LY-411575, 2 mg·kg^{-1}; Luteolin, 10 mg·kg^{-1}; LY + luteolin, LY-411575 (2 mg·kg^{-1}) + Luteolin (10 mg·kg^{-1}). $^{****}P < 0.0001$ *vs* control group; $^{\#}P < 0.05$, $^{\#\#\#}P < 0.001$, $^{\#\#\#\#}P < 0.000$ *vs* Model group; $^{\Delta}P < 0.05$, $^{\Delta\Delta\Delta\Delta}P < 0.0001$ *vs* LY group. Data are the mean ± SD.

portion of IL-17a^{+}ILC3 in UC mice administrated with Notch inhibitor LY-41157 is decreased, and the analysis of correlation results also showed that the proportion of NCR^{+}ILC3 was positively correlated with the proportion of IL-22^{+}ILC3, while the proportion of NCR^{+}ILC3 had none correlation with the proportion of IL-17a^{+}ILC3 (Figs. 5G–5L). Experiments *in vitro* showed that luteolin promoted the proportion of NCR^{+}MNK3, increased IL-22 level and decreased IL-17a level, due to the intervention of Notch inhibitor (LY-LY-411575), the effect of luteolin was prevented (Fig. 6). The results indicated that luteolin increased the proportion of NCR^{+}ILC3 was highly depended on Notch signaling pathway.

Notch signaling pathway in UC mice and the intervention of luteolin

since the non-redundant role of Notch signaling pathway in luteolin treating UC mice had been identified, we next monitored the Notch signaling in UC mice, on the one hand, to clarify the effect of luteolin on Notch signaling, and on the other hand, to test whether Notch inhibitor LY-411575 exerts

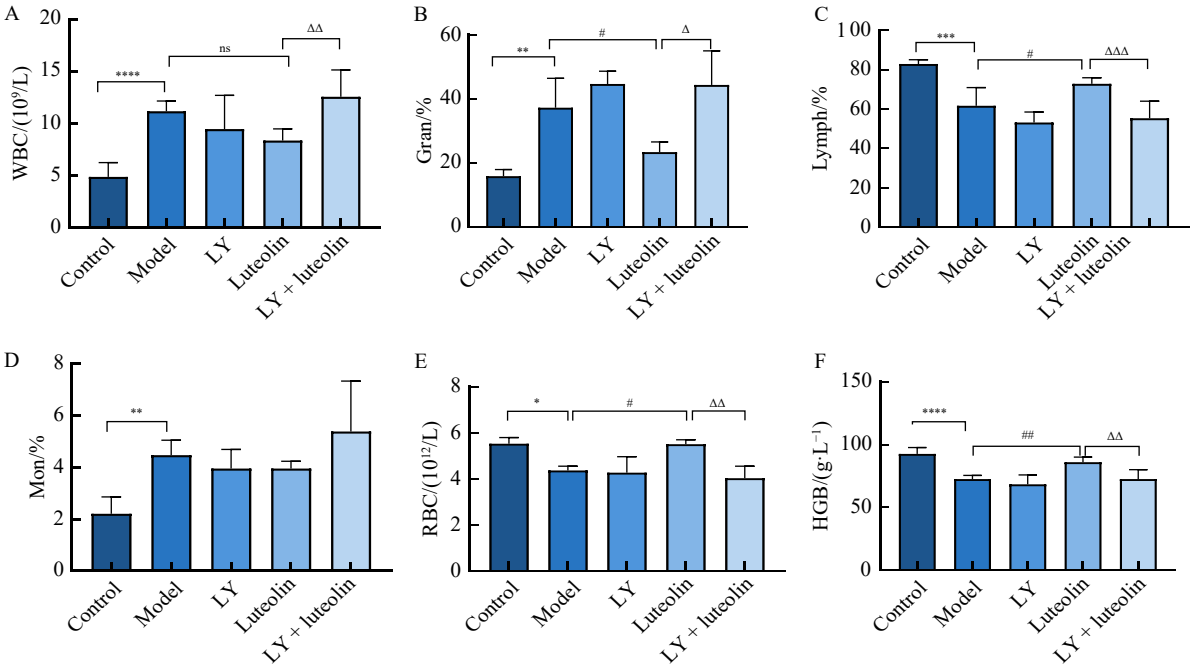

Fig. 3 Observation of peripheral blood cells in UC mice and intervention of luteolin. A, White blood cell (WBC) counts in peripheral blood (*n* = 6); B, The proportion of peripheral blood granulocytes (Gran%, *n* = 6); C, The proportion of peripheral blood lymphocytes (Lymph%, *n* = 6); D, The proportion of peripheral blood mononuclear cells (Mon%, *n* = 6); E, Red blood cell (RBC) counts in peripheral blood (*n* = 6); F, Hemoglobin (HGB) content in peripheral blood (*n* = 6). LY, Notch inhibitor, LY-411575, 2 mg·kg^{-1}; Luteolin, 10 mg·kg^{-1}; LY + luteolin, LY-411575 (2 mg·kg^{-1}) + Luteolin (10 mg·kg^{-1}). $^{*}P < 0.05$, $^{**}P < 0.01$, $^{***}P < 0.001$, $^{****}P < 0.0001$ *vs* control group; $^{\#}P < 0.05$, $^{\#\#}P < 0.01$ *vs* Model group; $^{\Delta}P < 0.05$, $^{\Delta\Delta}P < 0.01$, $^{\Delta\Delta\Delta}P < 0.001$, $^{\Delta\Delta\Delta\Delta}P < 0.0001$ *vs* LY group. Data are the mean ± SD.

its effect. Immunofluorescence results showed that colon Notch1 receptor protein and downstream target protein Hes1 fluorescence signals in UC mice and LY-411575 treated UC mice were weak, which was enhanced after luteolin treatment. However, this effect of luteolin was reversed after Notch signaling (γ-secretase inhibitor) was blocked (Figs. 7A−7B). WB results showed that LY-411575 treatment further blocked Notch signaling in UC mice. Although luteolin restored the abnormally blocked Notch signaling pathway in UC mice, it's fail to reverse the effect of LY-411575 (Figs. 7C−7F). The results revealed that luteolin activated Notch signaling pathway in UC mice.

Prediction of the target of luteolin action on Notch signaling pathway

Since it has been found that luteolin restored abnormally inhibited Notch signaling pathway in the colon of UC mice, considering that Notch signaling activation was involved in multiple complex aspects, we conducted molecular docking between luteolin and key proteins in the Notch signaling pathway to evaluate their affinity and binding sites. The molecular docking results of Luteolin and RBPJ (mus musculus) protein showed that luteolin 5-hydroxyl was bonded to LEU (C: 101) and ASN (C: 147) by hydrogen bond, 5'-hydroxyl was bonded to GLU (C: 120) and SER (C: 123) by hydrogen bond. In addition, luteolin B& C rings formed Pi-Alkyl interactions with PRO (C: 125) and B rings formed Pi-Cation interactions with LYS (C: 110). The affinity of luteolin with RBPJ (mus musculus) was −7.5 kcal·mol^{-1}, indicating high binding capacity (Fig. 8A). The affinity of luteolin with Notch1 (homo sapiens) and RBPJ (homo sapiens) was respectively −6.4 kcal·mol^{-1} and −7.7 kcal·mol^{-1}, indicating high binding capacity (Figs. 8B−8C).

Discussion

The clinical features of ulcerative colitis include but don't limit to diarrhea, mucous, pus and blood stools and weight loss. DAI score reflected weight loss, fecal characteristics and severity of stool blood in UC mice, DAI score was decreased with luteolin treatment. All the pharmacodynamics indicators in this article showed that luteolin ameliorated UC related symptoms. In fact, The ideal state of the drug delivery system in UC treatment is to deliver the drug to the inflamed colon at a maximum dose to minimize systemic drug exposure and reduce side effects. Yan etc.. developed two functionalized nanoparticle (NP) for efficient Pterostilbene (rapid plasma clearance) delivery to treat UC [24-25]. Although luteolin shows low bioavailability, applicable dosage form and drug delivery system are good at dealing with those problems.

It is worth noting that UC mice treated with Notch inhibitors showed mild symptoms in the early stages, but it's worsened at the third round of model. In fact, Notch signaling was activated in the incipient stage of tissue injury, which further aggravated the inflammatory response in mice [26-28].

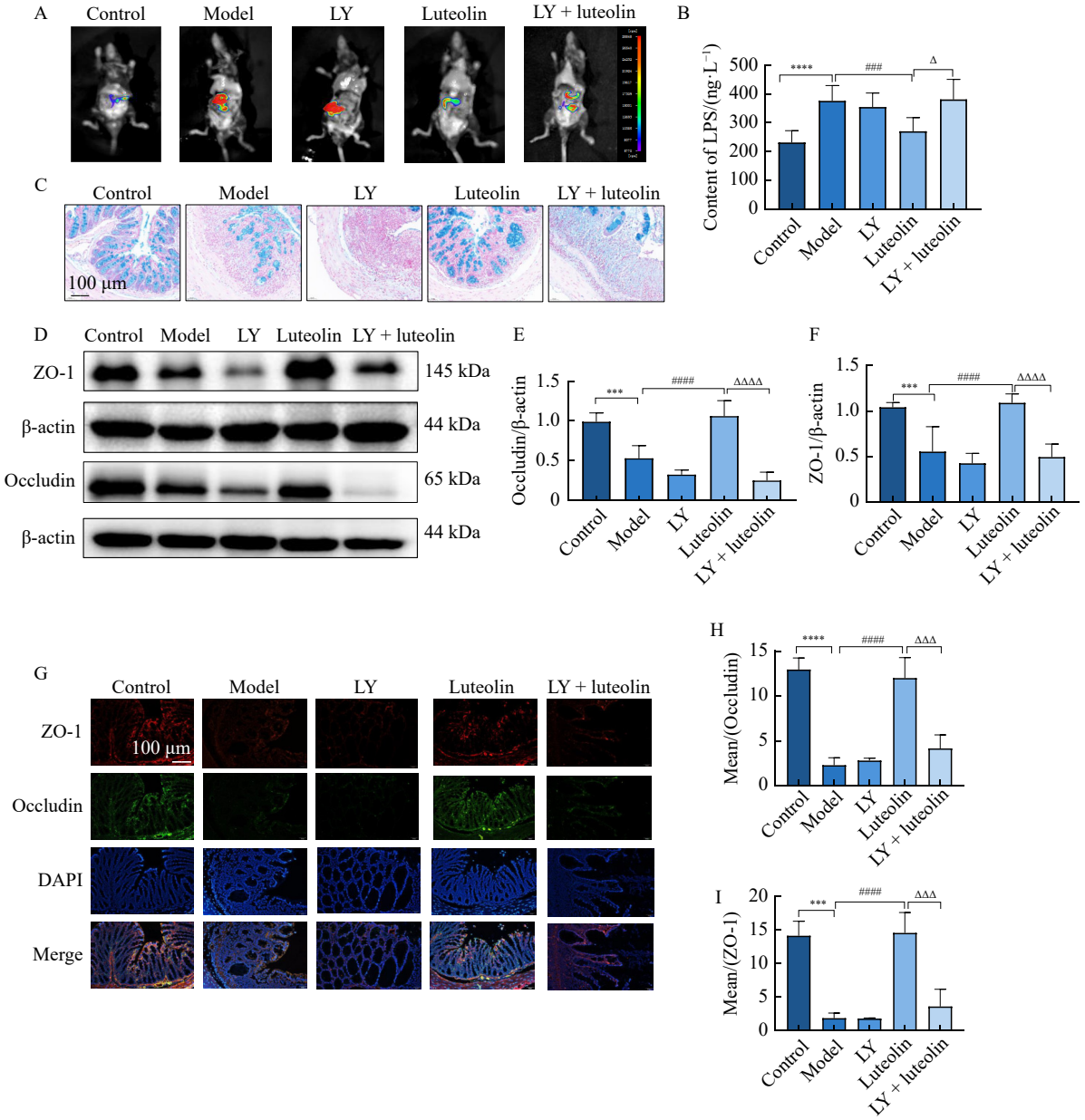

Fig. 4 Effect of luteolin on intestinal epithelial permeability in UC mice and intervention of LY-411575. A, Distribution of FITC-dextran was detected by small animal imaging (n = 3); B, content of LPS inplasma in UC mice (n = 9); C, Mucin (blue) was detected by alcian blue & nuclear fast red staining kit (200 ×, n = 6); D−F, Expression of ZO-1, Occludin proteins were determined by WB (n = 5); G−I, TJ proteins ZO-1, Occludin were observed by immunofluorescence (200 ×, n = 3) LY, Notch inhibitor, LY-411575, 2 mg·kg^{-1}; Luteolin, 10 mg·kg^{-1}; LY + luteolin, LY-411575 (2 mg·kg^{-1})+Luteolin (10 mg·kg^{-1}). $^{***}P < 0.001$, $^{****}P < 0.0001$ *vs* control group; $^{###}P < 0.001$, $^{####}P < 0.0001$ *vs* Model group; $^{Δ}P < 0.05$, $^{ΔΔΔ}P < 0.001$, $^{ΔΔΔΔ}P < 0.0001$ *vs* LY group. Data are the mean ± SD.

Therefore, inhibiting Notch signaling in the early stages of the inflammatory response actually improves the symptom of UC. In the later stage of injury or inflammation, the repair of intestinal epithelium requires up-regulation of Notch signaling pathway, which contributes to epithelial regeneration and enhances the barrier function of intestinal epithelium [29]. Therefore, Notch signaling is a double-edged sword in UC, activation or inhibition of Notch signaling pathway at the appropriate time provide beneficial effects on UC.

It is generally believed that abnormal intestinal epithelial barrier function precedes the occurrence of UC, and the abnormal differentiation and proliferation of intestinal epithelial cells is an important cause of the abnormal intestinal mucosal barrier function [30]. Notch pathway has been shown to be the key to guiding progenitor cell differentiation into absorbent and secretory cell fates [31]. Notch signaling pathway protects intestinal mucosal barrier function by promoting the expression of tight junction protein. Previous studies had shown that in mice intestinal or Caco-2 cells, the loss of Notch signal significantly reduced the expression of proteins

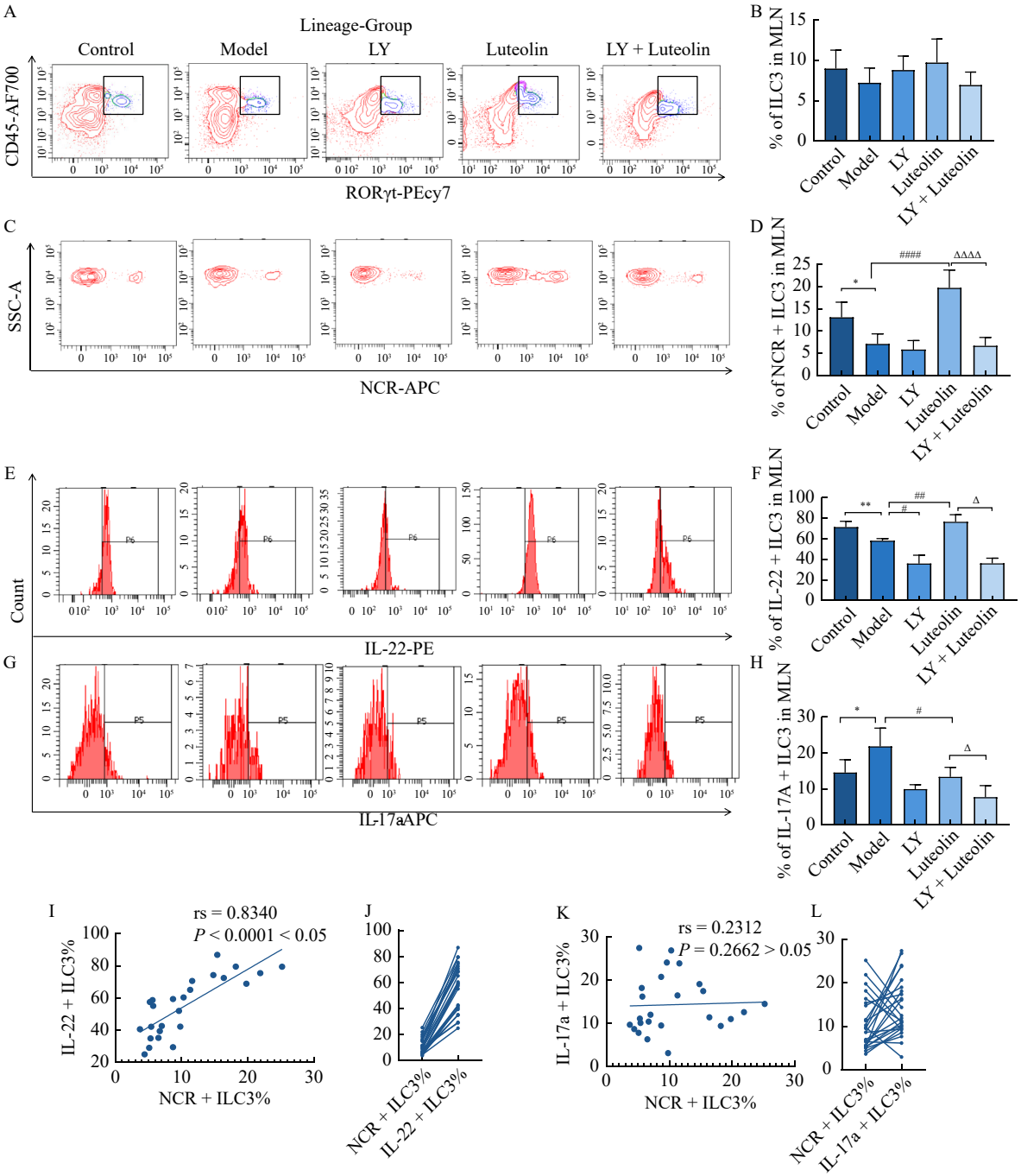

Fig. 5 Luteolin dependent Notch signaling increased the proportion of NCR$^+$ILC3 and IL-22$^+$ILC3 in UC mice. A&B, The proportion of ILC3 in UC mice were detected by flow cytometry (n = 5).; C&D The proportion of NCR$^+$ILC3 in UC mice were detected by flow cytometry (n = 5). E&F, The proportion of IL-22$^+$ILC3 in UC mice were detected by flow cytometry (n = 5). G&H, The proportion of IL-17a$^+$ILC3 in UC mice were detected by flow cytometry (n = 5). I&J, Correlation analysis between the proportion of NCR$^+$ILC3 and the proportion of IL-22$^+$ILC3 (n = 25); K&L, Correlation analysis between the proportion of NCR$^+$ILC3 and the proportion of IL-17a$^+$ILC3 (n = 25). LY, Notch inhibitor, LY-411575, 2 mg·kg^{-1}; Luteolin, 10mg·kg^{-1}; LY + luteolin, LY-411575 (2 mg·kg^{-1})+Luteolin (10 mg·kg^{-1}). $^*P < 0.05$, $^{**}P < 0.01$ *vs* control group; $^{\#}P < 0.05$, $^{\#\#}P < 0.01$, $^{\#\#\#\#}P < 0.0001$ *vs* Model group; $^{\Delta}P < 0.05$, $^{\Delta\Delta\Delta\Delta}P < 0.0001$ *vs* LY group. Data are the mean ± SD.

such as Occludin, ZO-1, Claudin-1 and Claudin-5, resulting in the imbalance of tight junction protein complex and the decrease in transepithelial resistance, finally, the intestinal barrier function is impaired [32-33].

Notch signaling pathway not only directly regulates the function and differentiation of intestinal epithelial cells but also maintains the function of the intestinal immune system. Our experiment proved that luteolin relies on Notch signaling to increase the proportion of NCR$^+$ILC3 in UC mice. The activation of Notch signaling in NCR$^+$ILC3 stimulates the ex-

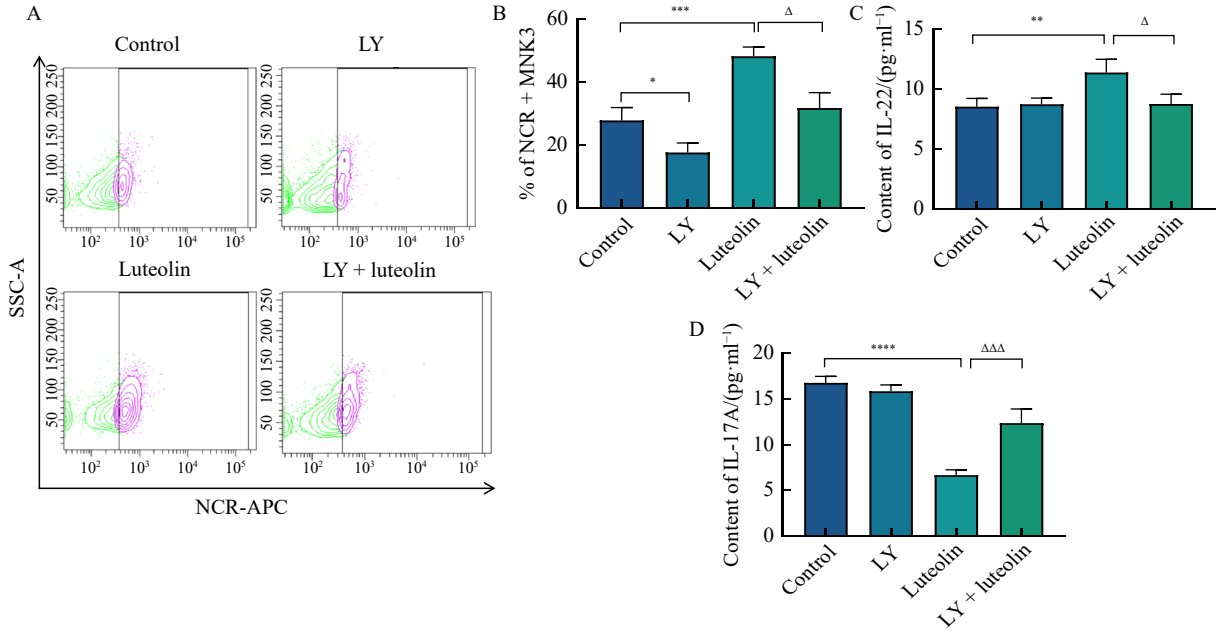

Fig. 6 Luteolin dependent Notch signaling increased the proportion of NCR$^+$MNK3. A&B, The proportion of NCR$^+$MNK3 in UC mice were detected by flow cytometry (n = 3). C, The content of IL-22 in MNK3 cells was detected by ELISA (n = 3). D, The content of IL-17A in MNK3 cells was detected by ELISA (n = 3). LY, Notch inhibitor, LY-411575, 2 μmol·L^{-1}; Luteolin, 3.125 μmol·L^{-1}; LY + luteolin, LY-411575 (2 μmol·L^{-1})+Luteolin (3.125 μmol·L^{-1}). $^*P < 0.05$, $^{**}P < 0.01$, $^{***}P < 0.001$, $^{****}P < 0.0001$ *vs* control group; $^{\Delta}P < 0.05$, $^{\Delta\Delta\Delta}P < 0.001$ *vs* LY + luteolin group. Data are the mean ± SD.

pression of T-bet, RORγt and AhR, which is conducive to the differentiation of NCR$^-$ILC3 into NCR$^+$ILC3 [11]. T-bet directs the expression of NKp46 (NCR), a natural cytotoxic receptor [34]. RORγt is a highly dependent nuclear transcription factor for ILC3, losing the expression of RORγt, NCR$^+$ILC3 will further differentiate into ex-ILC3 and secrete INF-γ [35]. AhR is essential for the development of ILC3 and regulates the expression of RORγt and the production of IL-22 [36]. It has been reported that activation of Notch signaling promoted the differentiation of naive CD4$^+$ T cells into Th22 cells, this is the key to T cells for the production of IL-22 [37-38]. In fact, ILC3 is functionally similar to Th17 and Th22, which secretes the Th17 and Th22-like cytokines IL-22, IL-17, and GM-CSF [39].

The role of IL-22 in promoting intestinal epithelial repair is well established [40]. The level of intestinal IL-22 was decreased in UC patients, and supplementation of exogenous IL-22 promoted the intestinal epithelium repairing to alleviate UC [41]. ILC3, especially NCR$^+$ILC3, is an important source of intestinal IL-22. We found that luteolin increased

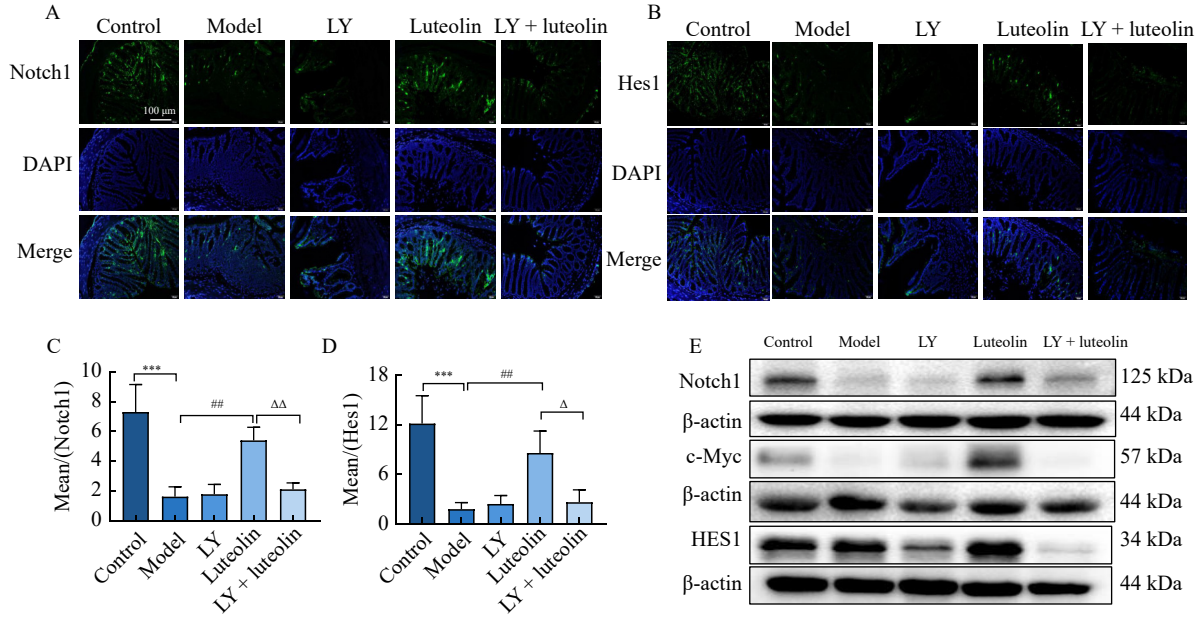

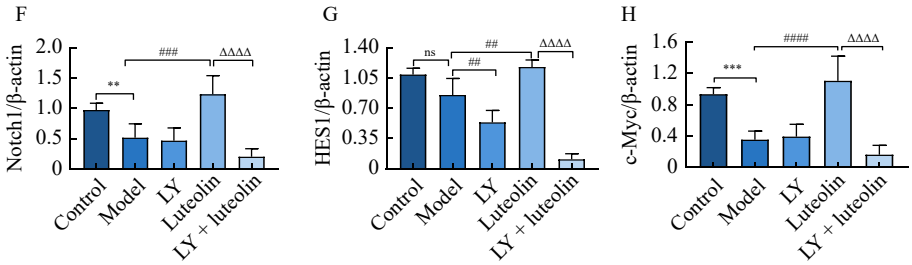

Fig. 7 Effect of luteolin on Notch signaling pathway in UC mice. A, Expression of Notch1 were observed by immunofluorescence (200 ×, *n* = 3); B, Expression of Hes1 were observed by immunofluorescence (200 ×, *n* = 3);C−D, fluorescence statistics of protein Notch1 and Hes1 with Image-J. E−H, Expression of Notch1, c-Myc and Hes1 proteins were determined by WB (*n* = 5). LY, Notch inhibitor, LY-411575, 2 mg·kg^{-1}; Luteolin, 10 mg·kg^{-1}; LY + luteolin, LY-411575 (2 mg·kg^{-1}) + Luteolin (10 mg·kg^{-1}). $^{**}P < 0.01$, $^{***}P < 0.001$ *vs* control group; $^{\#\#}P < 0.01$, $^{\#\#\#}P < 0.001$, $^{\#\#\#\#}P < 0.0001$ *vs* Model group; $^{\Delta\Delta\Delta\Delta}P < 0.0001$ *vs* LY group. Data are the mean ± SD.

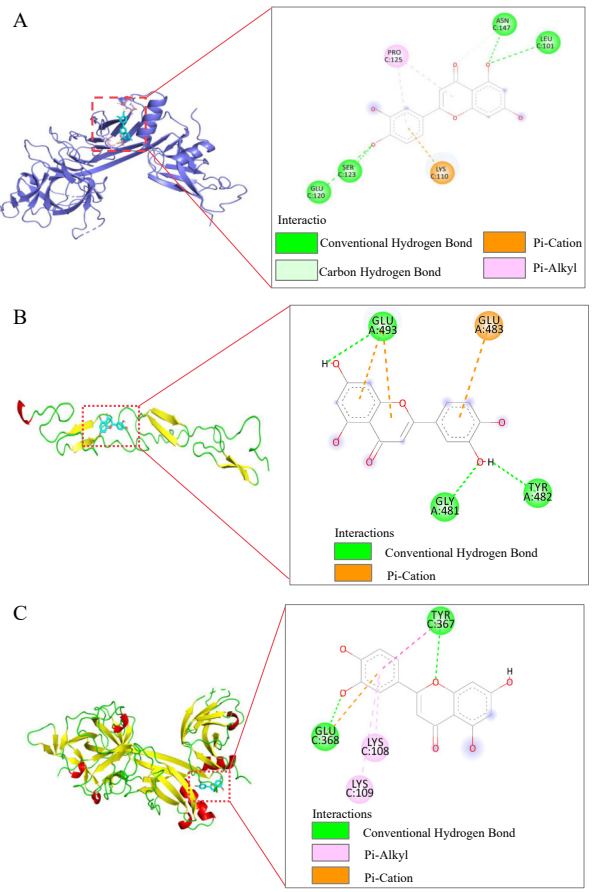

Fig. 8 Molecular docking and interaction profiling. A, Luteolin to the active-site cleft of mouse musculus RBPJ (affinity = −7.5 kcal·mol^{-1}); B, Luteolin to the active-site cleft of homo sapiens Notch1 (affinity = −6.4 kcal·mol^{-1}); C, Luteolin to the active-site cleft of homo sapiens RBPJ (affinity = −7.7 kcal·mol^{-1}).

the proportion of intestinal NCR^{+}ILC3 and IL-22^{+}ILC3 in UC mice. Analysis of correlation results showed that promoting the proportion of NCR^{+}ILC3 was conducive to the maintenance of IL-22 level in colon, which was favorable to the recovery of intestinal barrier function after colon injury. IL-22 promoted the differentiation of mucus-producing goblet cells and participated in the formation of the mucous layer [42]; IL-22 stimulated intestinal epithelium and Paneth cells to produce high levels of antimicrobial peptides and maintained intestinal homeostasis [43]; IL-22 enhanced the tight junction protein and other mechanisms to promote intestinal epithelium repairing [44]; IL-22 promoted the proliferation of Ki67^{+}intestinal epithelial cells *via* affecting the development of Lgr5^{+}ISCs to repair the epithelium [45].

It had been reported that NCR^{-}ILC3 is dominant in UC, which incured spontaneous colitis and bacteria-driven colitis by secreting IL-17a [46]. IL-17a induced epithelial cells and endothelial cells to release chemokines and infiltrated a large number of inflammatory cells into the inflammatory site, resulting in the breakdown of intestinal epithelial tight connections, the increase of intestinal permeability, a large number of antigens invading the intestinal barrier, over-activation of immune response, and aggravation of inflammation [12]. although our experimental results showed that there was no correlation between the proportion of NCR^{+}ILC3 and the proportion of IL-17a^{+}ILC3, which showed a negative correlation after deleting the data of LY group and LY + luteolin group (Supplementary Fig.2). This suggested that inhibition of Notch signaling regulated ILC3 secreting IL-17a *via* other ways.

LY-411575 is a potent γ-secretase inhibitor [17-18]. The γ-secretase produces the second cleavage event at the S3 site of Notch transmembrane domain, resulting in the release of the Notch intracellular domain (NICD), which is subsequently transferred to the nucleus to bind to RBPJ, thereby activating downstream target genes [47]. Luteolin didn't promote the expression of Notch signal pathway downstream proteins Hes1 and c-Myc after blocking gamma-secretase, which suggested that luteolin didn't target γ-secretase. At the same time, the results of molecular docking predicted that luteolin had good binding ability with Notch1 receptor and RBPJ in both mouse and Homo sapiens. In fact, there are many emerging technologies such as single-cell multiomics, network pharmacology, and artificial intelligence in the pharmacological studies of natural products to provide insights for the development of innovative natural product-based drugs [48-49]. In brief, our study have shown that Notch signaling is expected to be a po-

tential target for luteolin in UC treatment strategies in future.

Conclusion

To the best of our knowledge, this is the first description of the non-redundant role of Notch signaling pathway on luteolin ameliorating ulcerative colitis in mice through enhancing the proportion of NCR$^+$ILC3. Intestinal mucosal repair is the latest strategy for the treatment of ulcerative colitis (UC). IL-22 is a key cytokine to promote mucosal repair, and the level of IL-22 mainly depends on NCR$^+$ILC3, so maintaining the number and function of NCR$^+$ILC3 is favorable to promote UC mucosal repair. In this study, mucosal repairing was taken as the starting point, and the immune mechanism of luteolin improving UC by maintaining the amount of NCR$^+$ILC3 was investigated thoroughly, and on this basis, the role of NCR$^+$ILC3 in UC was further perspicuous.All the results show that Notch signaling was down-regulated in UC mice, and luteolin targeted Notch signaling pathway and promoted the proportion of NCR$^+$ILC3 to enhance the level of IL-22.

References

[1] Huang LJ, Mao XT, Li YY, *et al*. Multiomics analyses reveal a critical role of selenium in controlling T cell differentiation in Crohn's disease [J]. *Immunity*, 2021, **54**(8): 1728-1744.e7.

[2] Kotla NG, Rochev Y. IBD disease-modifying therapies: insights from emerging therapeutics [J]. *Trends Mol Med*, 2023, **29**(3): 241-253.

[3] Pellicciotta M, Rigoni R, Falcone EL, *et al*. The microbiome and immunodeficiencies: lessons from rare diseases [J]. *J Autoimmun*, 2019, **98**(undefined): 132-148.

[4] Corley DA, Schuppan D. Food, the immune system, and the gastrointestinal tract [J]. *Gastroenterology*, 2015, **148**(6): 1083-1086.

[5] Odenwald MA, Turner JR. The intestinal epithelial barrier: a therapeutic target? [J]. *Nat Rev Gastroenterol Hepatol*, 2017, **14**(1): 9-21.

[6] Maloy KJ, Powrie F. Intestinal homeostasis and its breakdown in inflammatory bowel disease [J]. *Nature*, 2011, **474**(7351): 298-306.

[7] Keir M, Yi TS, Lu T, *et al*. The role of IL-22 in intestinal health and disease [J]. *J Exp Med*, 2020, **217**(3): e20192195.

[8] Tsai PY, Zhang BK, He WQ, *et al*. IL-22 upregulates epithelial claudin-2 to drive diarrhea and enteric pathogen clearance [J]. *Cell Host Microbe*, 2017, **21**(6): 671-681.e4.

[9] Takatori H, Kanno Y, Watford WT, *et al*. Lymphoid tissue inducer-like cells are an innate source of IL-17 and IL-22 [J]. *J Exp Med*, 2009, **206**(1): 35-41.

[10] Croft CA, Thaller A, Marie S, *et al*. Notch, RORC and IL-23 signals cooperate to promote multi-lineage human innate lymphoid cell differentiation [J]. *Nat Commun*, 2022, **13**(1): 4344.

[11] Chea S, Perchet T, Petit M, *et al*. Notch signaling in group 3 innate lymphoid cells modulates their plasticity [J]. *Sci Signal*, 2016, **9**(426): ra45.

[12] Chang Y, Kim JW, Yang S, *et al*. Increased GM-CSF-producing NCR ILC3s and neutrophils in the intestinal mucosa exacerbate inflammatory bowel disease [J]. *Clin Transl Immunol*, 2021, **10**(7): e1311.

[13] Goc J, Lv M, Bessman NJ, *et al*. Dysregulation of ILC3s unleashes progression and immunotherapy resistance in colon cancer [J]. *Cell*, 2021, **184**(19): 5015-5030.e16.

[14] Nong FF, Zhao ZX, Luo X, *et al*. Evaluation of the influence of mirabilite on the absorption and pharmacokinetics of the ingredients in Dahuang-mudan Decoction by a validated UPLC/QTOF-MS/MS method [J]. *Biomed Chromatogr*, 2019, **33**(3): e4423.

[15] Huang SW, Wang XJ, Xie XQ, *et al*. Dahuang Mudan Decoction repairs intestinal barrier in chronic colitic mice by regulating the function of ILC3 [J]. *J Ethnopharmacol*, 2022, **299**(undefined): 115652.

[16] Xie XQ, Zhao M, Huang SW, *et al*. Luteolin alleviates ulcerative colitis by restoring the balance of NCR$^-$ILC3/NCR$^+$ ILC3 to repairing impaired intestinal barrier [J]. *Int Immunopharmacol*, 2022, **112**(undefined): 109251.

[17] Otoguro T, Tanaka T, Kasai H, *et al*. Inhibitory effect of presenilin inhibitor LY411575 on maturation of hepatitis C virus core protein, production of the viral particle and expression of host proteins involved in pathogenicity [J]. *Microbiol Immunol*, 2016, **60**(11): 740-753.

[18] Hyde LA, McHugh NA, Chen J, *et al*. Studies to investigate the *in vivo* therapeutic window of the gamma-secretase inhibitor N2-[(2*S*)-2-(3, 5-difluorophenyl)-2-hydroxyethanoyl]-N1-[(7*S*)-5-methyl-6-oxo-6, 7-dihydro-5H-dibenzo[b, d]azepin-7-yl]-L-alaninamide (LY411, 575) in the CRND8 mouse [J]. *J Pharmacol Exp Ther*, 2006, **319**(3): 1133-1143.

[19] Zhang JJ, Yuan GQ, Dong MC, *et al*. Notch signaling modulates proliferative vitreoretinopathy *via* regulating retinal pigment epithelial-to-mesenchymal transition [J]. *Histochem Cell Biol*, 2017, **147**(3): 367-375.

[20] Friedmann DR, Kovall RA. Thermodynamic and structural insights into CSL-DNA complexes [J]. *Protein Sci*, 2010, **19**(1): 34-46.

[21] Li ZJ, Han K, Pak JE, *et al*. Recognition of EGF-like domains by the Notch-modifying O-fucosyltransferase POFUT1 [J]. *Nat Chem Biol*, 2017, **13**(7): 757-763.

[22] Landor SKJ, Santio NM, Eccleshall WB, *et al*. PIM-induced phosphorylation of Notch3 promotes breast cancer tumorigenicity in a CSL-independent fashion [J]. *J Biol Chem*, 2021, **296**(undefined): 100593.

[23] Taylor P, Takeuchi H, Sheppard D, *et al*. Fringe-mediated extension of O-linked fucose in the ligand-binding region of Notch1 increases binding to mammalian Notch ligands [J]. *Proc Natl Acad Sci U S A*, 2014, **111**(20): 7290-7295.

[24] Yan XJ, Meng LZ, Zhang XZ, *et al*. Reactive oxygen species-responsive nanocarrier ameliorates murine colitis by intervening colonic innate and adaptive immune responses [J]. *Mol Ther*, 2023, **31**(5): 1383-1401.

[25] Wei W, Zhang YJ, Li RQ, *et al*. Oral delivery of pterostilbene by L-arginine-mediated "Nano-Bomb" carrier for the treatment of ulcerative colitis [J]. *Int J Nanomedicine*, 2022, **17**(undefined): 603-616.

[26] Holmberg FE, Seidelin JB, Yin XL, *et al*. Culturing human intestinal stem cells for regenerative applications in the treatment of inflammatory bowel disease [J]. *EMBO Mol Med*, 2017, **9**(5): 558-570.

[27] Van der SM, De KBAE, De BACJM, *et al*. Muc2-deficient mice spontaneously develop colitis, indicating that MUC2 is critical for colonic protection [J]. *Gastroenterology*, 2006, **131**(1): 117-129.

[28] Zhao YX, Luan HF, Gao H, *et al*. Gegen Qinlian Decoction maintains colonic mucosal homeostasis in acute/chronic ulcerative colitis *via* bidirectionally modulating dysregulated Notch signaling [J]. *Phytomedicine*, 2020, **68**(undefined): 153182.

[29] Wang YW, Huang D, Chen KY, *et al*. Fucosylation deficiency in mice leads to colitis and adenocarcinoma [J]. *Gastroentero-*

logy, 2017, **152**(1): 193-205.
[30] Wang X, Ni JH, You Y, *et al*. SNX10-mediated LPS sensing causes intestinal barrier dysfunction *via* a caspase-5-dependent signaling cascade [J]. *EMBO J*, 2021, **40**(24): e108080.
[31] Troll JV, Hamilton MK, Abel ML, *et al*. Microbiota promote secretory cell determination in the intestinal epithelium by modulating host Notch signaling [J]. *Development*, 2018, **145**(4): undefined.
[32] Mathern DR, Laitman LE, Hovhannisyan Z, *et al*. Mouse and human Notch-1 regulate mucosal immune responses [J]. *Mucosal Immunol*, 2014, **7**(4): 995-1005.
[33] Pope JL, Bhat AA, Sharma A, *et al*. Claudin-1 regulates intestinal epithelial homeostasis through the modulation of Notch-signalling [J]. *Gut*, 2014, **63**(4): 622-634.
[34] Rankin LC, Groom JR, Chopin M, *et al*. The transcription factor T-bet is essential for the development of NKp46$^+$ innate lymphocytes *via* the Notch pathway [J]. *Nat Immunol*, 2013, **14**(4): 389-395.
[35] Ishizuka IE, Chea S, Gudjonson H, *et al*. Single-cell analysis defines the divergence between the innate lymphoid cell lineage and lymphoid tissue-inducer cell lineage [J]. *Nat Immunol*, 2016, **17**(3): 269-276.
[36] Li YY, Wang XJ, Su YL, *et al*. Baicalein ameliorates ulcerative colitis by improving intestinal epithelial barrier *via* AhR/IL-22 pathway in ILC3s [J]. *Acta Pharmacol Sin*, 2022, **43**(6): 1495-1507.
[37] Wei X, Wang JP, Hao CQ, *et al*. Notch signaling contributes to liver inflammation by regulation of interleukin-22-producing cells in hepatitis B virus infection [J]. *Front Cell Infect Microbiol*, 2016, **6**(undefined): 132.
[38] Sukhotnik I, Coran AG, Pollak Y, *et al*. Activated Notch signaling cascade is correlated with stem cell differentiation toward absorptive progenitors after massive small bowel resection in a rat [J]. *Am J Physiol Gastrointest Liver Physiol*, 2017, **313**(3): G247-G255.
[39] Zeng B, Shi SN, Ashworth G, *et al*. ILC3 function as a double-edged sword in inflammatory bowel diseases [J]. *Cell Death Dis*, 2019, **10**(4): 315.
[40] Lindemans CA, Calafiore M, Mertelsmann AM, *et al*. Interleukin-22 promotes intestinal-stem-cell-mediated epithelial regeneration [J]. *Nature*, 2015, **528**(7583): 560-564.
[41] Wang BM, Lim JH, Kajikawa T, *et al*. Macrophage β2-integrins regulate IL-22 by ILC3s and protect from lethal citrobacter rodentium-induced colitis [J]. *Cell Rep*, 2019, **26**(6): 1614-1626.e5.
[42] Gulhane M, Murray L, Lourie R, *et al*. High fat diets induce colonic epithelial cell stress and inflammation that is reversed by IL-22 [J]. *Sci Rep*, 2016, **6**: 28990.
[43] Mukherjee S, Hooper LV. Antimicrobial defense of the intestine [J]. *Immunity*, 2015, **42**(1): 28-39.
[44] Yu L, Wang FJ, Cui YF, *et al*. Molecular characteristics of rhesus macaque interleukin-22: cloning, *in vitro* expression and biological activities [J]. *Immunology*, 2018, **154**(4): 651-662.
[45] Zwarycz B, Gracz AD, Rivera KR, *et al*. IL22 inhibits epithelial stem cell expansion in an ileal organoid model [J]. *Cell Mol Gastroenterol Hepatol*, 2019, **7**(1): 1-17.
[46] Powell N, Walker AW, Stolarczyk E, *et al*. The transcription factor T-bet regulates intestinal inflammation mediated by interleukin-7 receptor$^+$ innate lymphoid cells [J]. *Immunity*, 2012, **37**(4): 674-684.
[47] Shang YL, Smith S, Hu XY. Role of Notch signaling in regulating innate immunity and inflammation in health and disease [J]. *Protein Cell*, 2016, **7**(3): 159-74.
[48] Lu MK, Yin JY, Zhu Q, *et al*. Artificial intelligence in pharmaceutical sciences [J]. *Engineering*, 2023, **2023**.
[49] Zhu YY, Ouyang ZJ, Du HJ, *et al*. New opportunities and challenges of natural products research: when target identification meets single-cell multiomics [J]. *Acta Pharm Sin B*, 2022, **12**(11): 4011-4039.

Cite this article as: XIE Xueqian, LI Pengcheng, ZHAO Meng, *et al*. Luteolin ameliorates ulcerative colitis in mice *via* reducing the depletion of NCR$^+$ILC3 through Notch signaling pathway [J]. *Chin J Nat Med*, 2024, **22**(11): 991-1002.